Supporting Information

Colloidal hydroxyethyl starch for tumor targeted platinum delivery

Chen Xiao[a,b,#], Hang Hu[a,b,#], Hai Yang[a,b,#], Si Li[a,b], Hui Zhou[b], Jian Ruan[c], Yuting Zhu[c], Xiangliang Yang[a,b,d], Zifu Li[a,b,d,e*]

[a]National Engineering Research Center for Nanomedicine, College of Life Science and Technology, Huazhong University of Science and Technology, Wuhan, 430074, China

[b]Department of Nanomedicine and Biopharmaceutics, College of Life Science and Technology, Huazhong University of Science and Technology, Wuhan, 430074, China

[c]Wuhan HUST Life Science & Technology Co., Ltd, Wuhan, 430223, China

[d]Hubei Key Laboratory of Bioinorganic Chemistry and Materia Medica, Huazhong University of Science and Technology, Wuhan, 430074, China

[e]Wuhan Institute of Biotechnology, High Tech Road 666, East Lake High Tech Zone, Wuhan, 430040, China

Author Contributions:

[#]These three authors contributed equally to this work.

*Corresponding authors:

Professor Zifu Li

Tel.: 86 27 87792234, Fax: 86 27 87792234, E-mail: zifuli@hust.edu.cn

The gel permeation chromatography (GPC) with differential refractive index (DRI) detector was used to determine the molecular weight of HES samples.

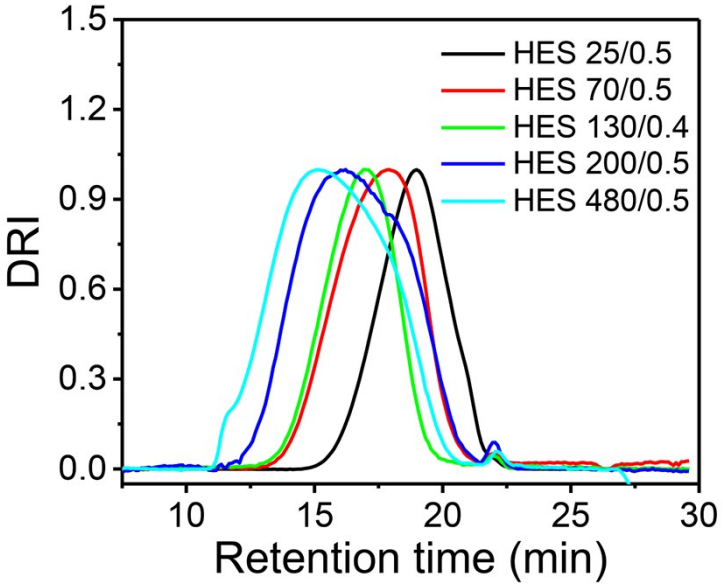

Figure S1. GPC traces of HES with different molecular weight.

The root mean square (RMS) of gyration radius (R_g) can also be obtained with GPC test by laser detector, and the molar mass were calculated according to the GPC spectra as shown in Figure S1. A double logarithmic plot of the RMS radius versus molar mass for different HES samples was plotted and shown in Figure S2. According to the equation (2) in the article, a linear fit was applied to each sample to calculate the conformational coefficient α.

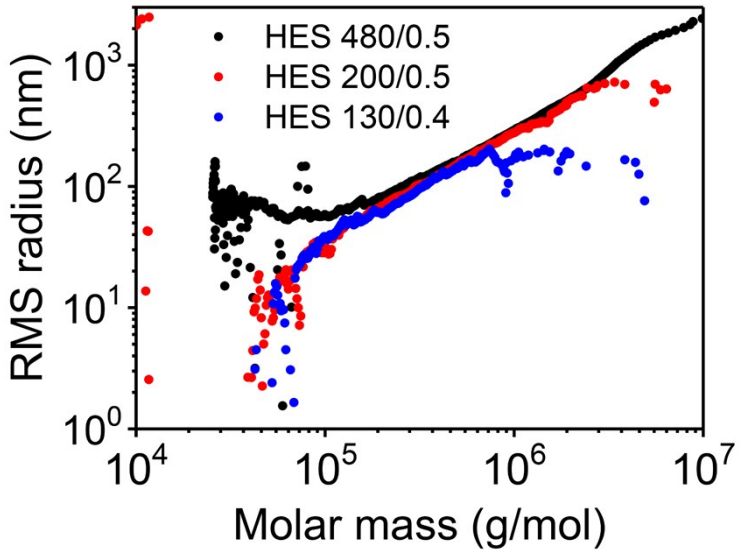

Figure S2. A double logarithmic plot of the RMS radius versus molar mass for different HES samples.

The structure of HES

By analyzing the ^{1}H NMR spectra of HES in deuterated water, key parameters, such as degree of branching (DB), molar substitution of hydroxyethyl (MS), and C_2/C_6 ratio of HES can be obtained. Peaks in ^{1}H NMR spectra between 4.8 ppm and 6.0 ppm can be assigned to H_1 (1-6) (4.89 ppm), H_1 (1-4) (5.33 ppm), H_1 (C_6 hydroxyethylated) (5.47 ppm), and H_1 (C_2 hydroxyethylated) (5.60 ppm), Figure S3 A and Figure S4. Therefore, C_2/C_6 ratio, degree of branching (DB), and molar substitution of hydroxyethyl (MS) of HES can be calculated according to the following formulas, respectively:

$$DB = \frac{H_1\,(1\text{-}6)}{Total\,H_1} \tag{2}$$

$$MS = \frac{H_1\left(C_2\,hydroxyethylated\right) + H_1\,(C_6\,hydroxyethylated)}{Total\,H_1} \tag{3}$$

$$C_2/C_6 = \frac{H_1\,(C_2\,hydroxyethylated)}{H_1\left(C_6\,hydroxyethylated\right)} \tag{4}$$

The MS and C_2/C_6 ratio are very important parameters, which control the *in vivo* α-amylase mediated degradation of HES. As previous reported, the MS and C_2/C_6 ratio of HES can be measured by many complex methods, such as gas chromatography (GC) and gas chromatography-mass spectrometer (GC-MS).[1, 2] Here we provide a simple method to determine the MS and C_2/C_6 ratio of HES. According to the Table 3, molar substitution of hydroxyethyl of HES 130/0.4 and 480/0.5 determined by equation (5) are consistent with the standard parameter. However, the MS of HES 25/0.5, 70/0.5 and 200/0.5 determined by this method are lower than the standard parameter. This may be because the fact that the ethoxyl etherification can take place not only in the glucose unit but also in the hydroxyethyl group, which may generate oligoethylene glycol group. In

addition, if ethoxyl etherification take place in the different site of the same glucosamine unit simultaneously, it may also cause the lower MS than the standard parameter. The C_2/C_6 ratio of our HES samples are around 3, as determined by equation (6). It is reported that the C_2/C_6 ratio of the commercial HES 200/0.5, 130/0.4 and 70/0.5 are 5, 9, 3 respectively.[1] The lower C_2/C_6 ratio indicates the faster clearance rate *in vivo*. The degree of branching of HES is defined as the percentage of α 1-6 glycosidic linkages in the total glycosidic linkages. The main chain of HES consists of α 1-4 glycosidic linkage and α 1-6 glycosidic linkage, which forms the branched chain. The degree of branching is related to the source of raw starch. It reveals that the degree of branching of our HES samples are between 5.5 % and 6 %, Table 3, which are very close to those reported by Besheer et al. The FT-IR spectra of HES show that there is a strong band at 3312 cm^{-1} which belongs to the stretch vibration of O-H of hydroxyl group, Figure S3 B. HES has plenty of hydroxyl groups for chemical modifications.[3-5] Based on the above characterization, a schematic graph of the structure of HES was proposed (Figure S3 C and D). According to the ^1H NMR spectra, the degree of branching of HES are around 6%, which mean that there is one branch site followed by 17 linear glucose units. Meanwhile, taking MS and C_2/C_6 ratio into consideration, there are 1204 glucose units, and 602 hydroxyethyl groups among a single HES 200/0.5 molecular, 3/4 of hydroxyethyl groups at C_2 site, 1/4 at C_6 site. Both conformational coefficient α and ρ-ratio corroborate HES adopt a compact conformation between dendrimers and hyper-branched polymer. Together, HES is a hyperbranched polymer, and there are many hydroxyl sites that can be modified.

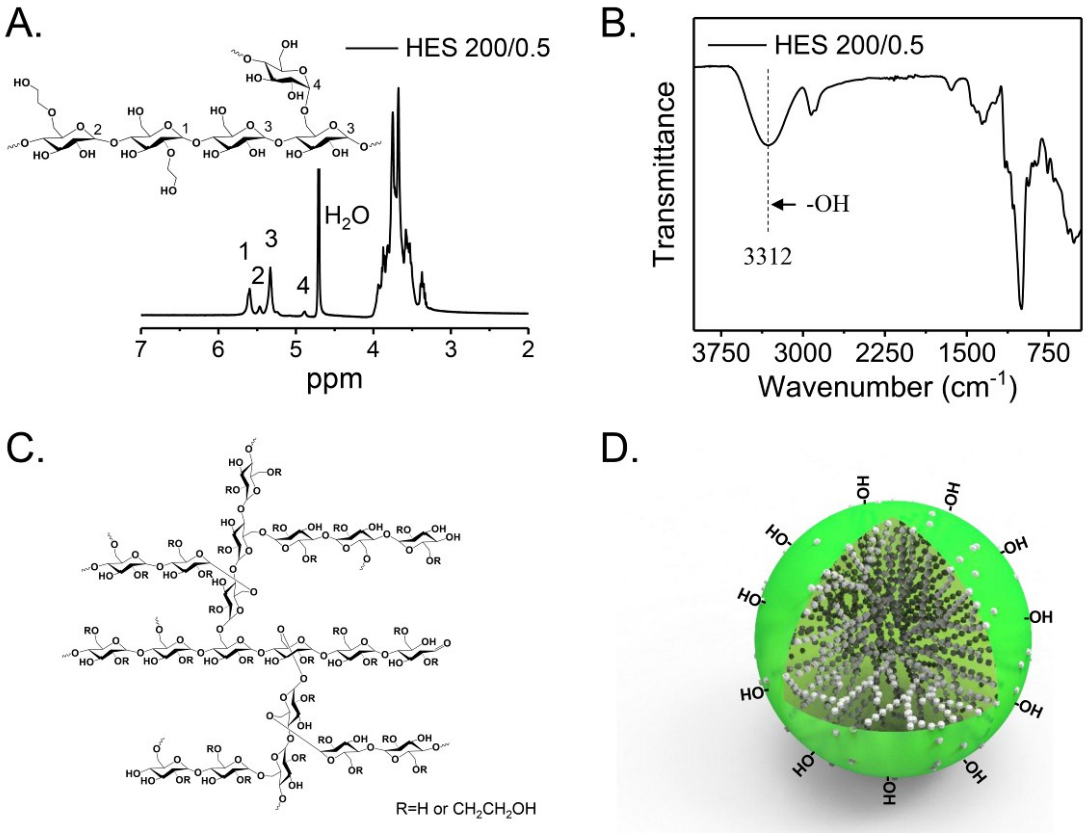

Figure S3. Characterization of HES. (A) ^{1}H-NMR spectra of HES 200/0.5. (B) FT-IR spectra of HES 200/0.5. (C) molecular formula and (D) 3D schematic illustration of the structure of HES.

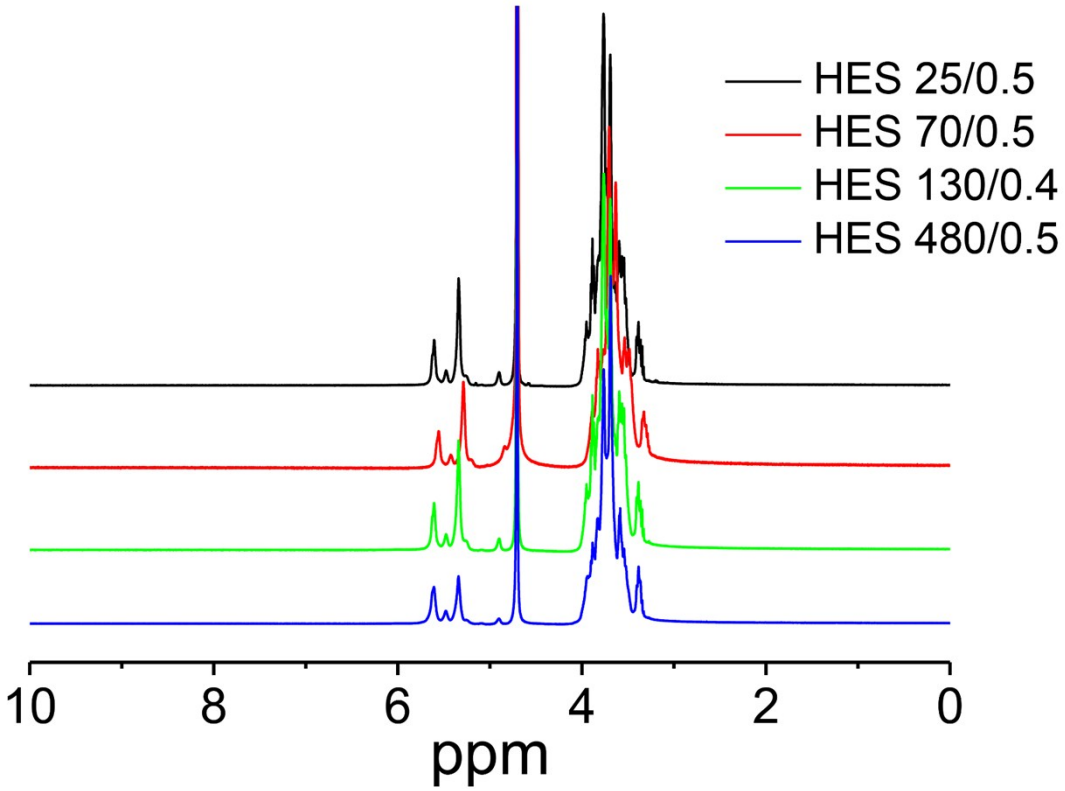

Figure S4. ^{1}H-NMR spectra of various HES in D_2O.

The colloid properties of HES

In the colloidal solution of HES, the osmotic pressure is an important parameter used in clinical plasma expansion. However, the influence of solution osmotic pressure on HES size is seldom investigated. Therefore, the relationship between osmotic pressure and size of HES was studied here, Figure S5. The osmotic pressure is positive correlated with the concentration. It can be obtained with the following equation:

$$\pi = cRT \quad (1)$$

where π stands for osmotic pressure, c is the concentration, R is the constant, T is temperature. The hydrodynamic diameter of HES decreases with increasing concentration, suggesting the hydrodynamic diameter of HES is dependent on the osmatic pressure. This is the first time that HES has been found to have this property. Figure S5 implies that HES are soft nanoparticles which can be squeezed under external stress. This may be used in cancer drug delivery system to take advantage of the high interstitial pressure for deep penetration. Figure S5 also reminds us to specify the concentration of HES when we report the hydrodynamic dimater results of HES with DLS. Otherwise, it is useless to compare results from different groups even though they use the exact same brand sample.

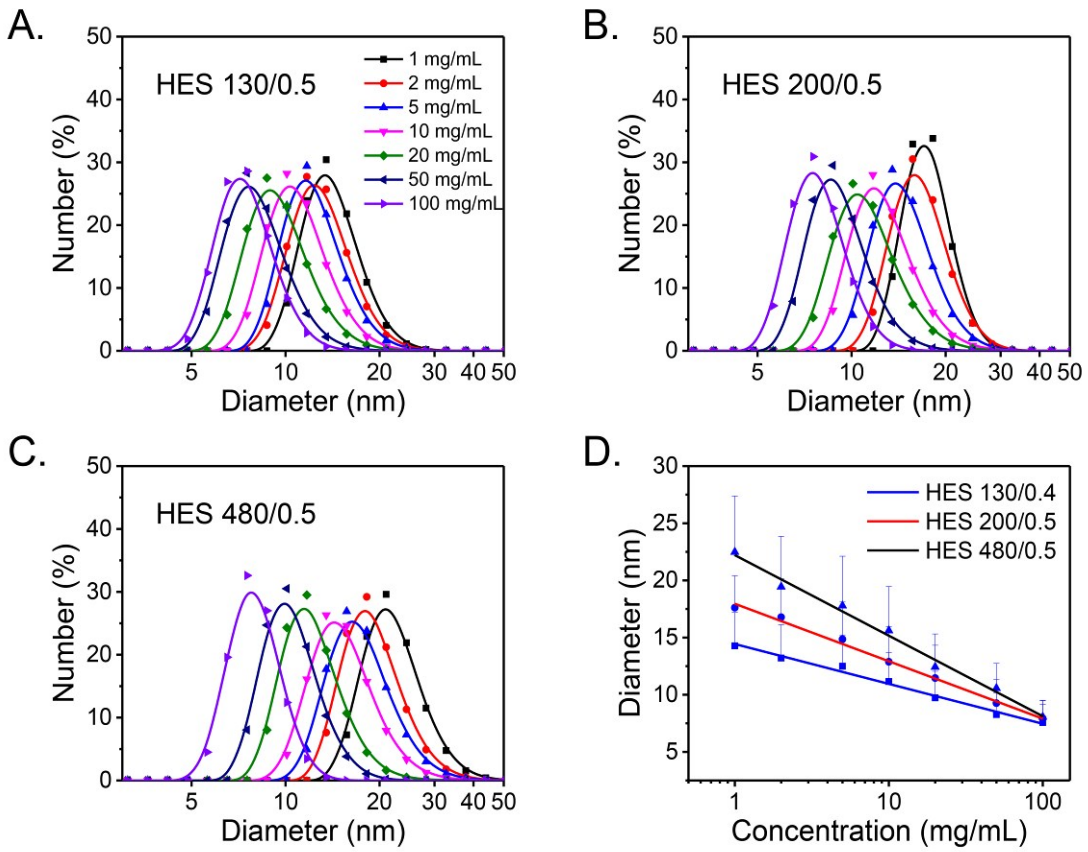

Figure S5. Size distribution of HES 130/0.4 (A), HES 200/0.5 (B), and HES 480/0.5 (C) at various concentration. Diameter of HES 130/0.4, HES 200/0.5, and HES 480/0.5 as a function of concentration (D).

The ^{1}H-NMR and FT-IR spectra of Pt-COOH are consistent with previous reports,[6, 7] indicating the success synthesis of Pt-COOH, Figure S6 A and B. The UV spectra of cis-platinum changed after being oxidized by H_2O_2 and modified with carboxyl group, Figure S6 C. The UV spectra of HES-Pt and LA-HES-Pt are quite different from HES, while similar to Pt-COOH, indicating that Pt-COOH is successfully conjugated onto HES.

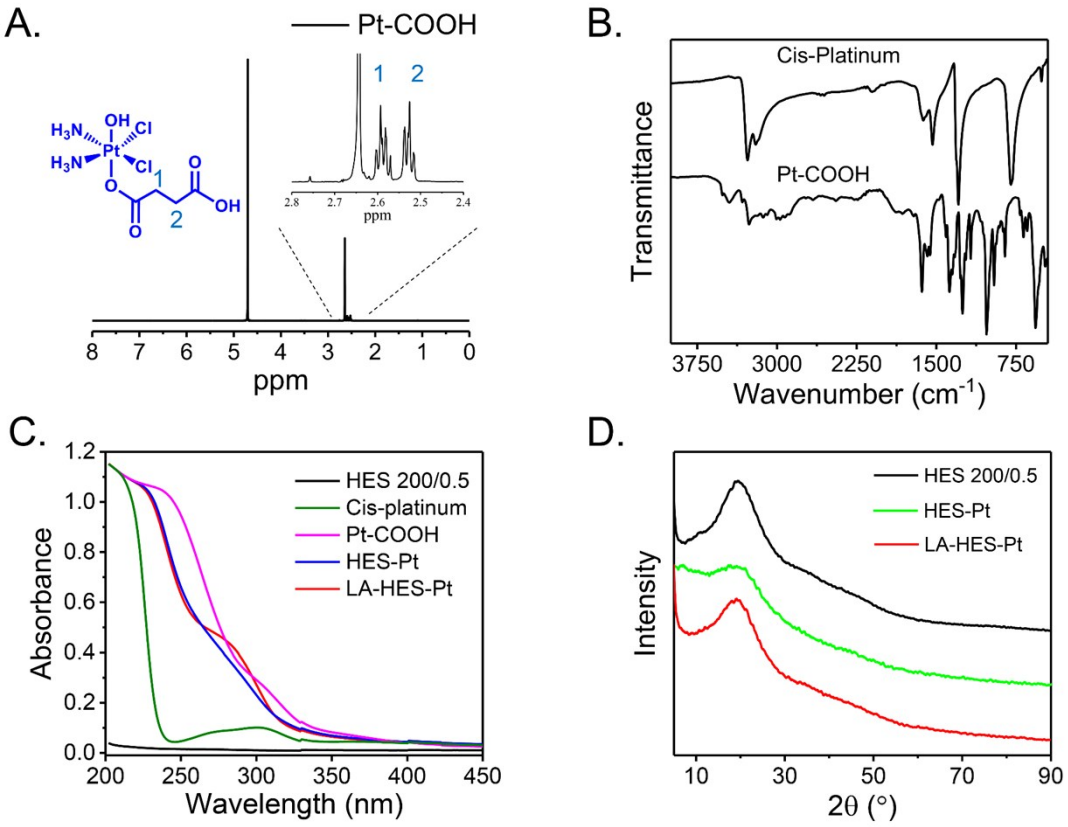

Figure S6. (A) ^{1}H-NMR spectra of Pt-COOH. (B) FT-IR spectra of Cis-platinum and Pt-COOH. (C) UV-vis spectra of HES, Cis-platinum, Pt-COOH, HES-Pt, and LA-HES-Pt. (D) XRD patterns of HES, HES-Pt and LA-HES-Pt.

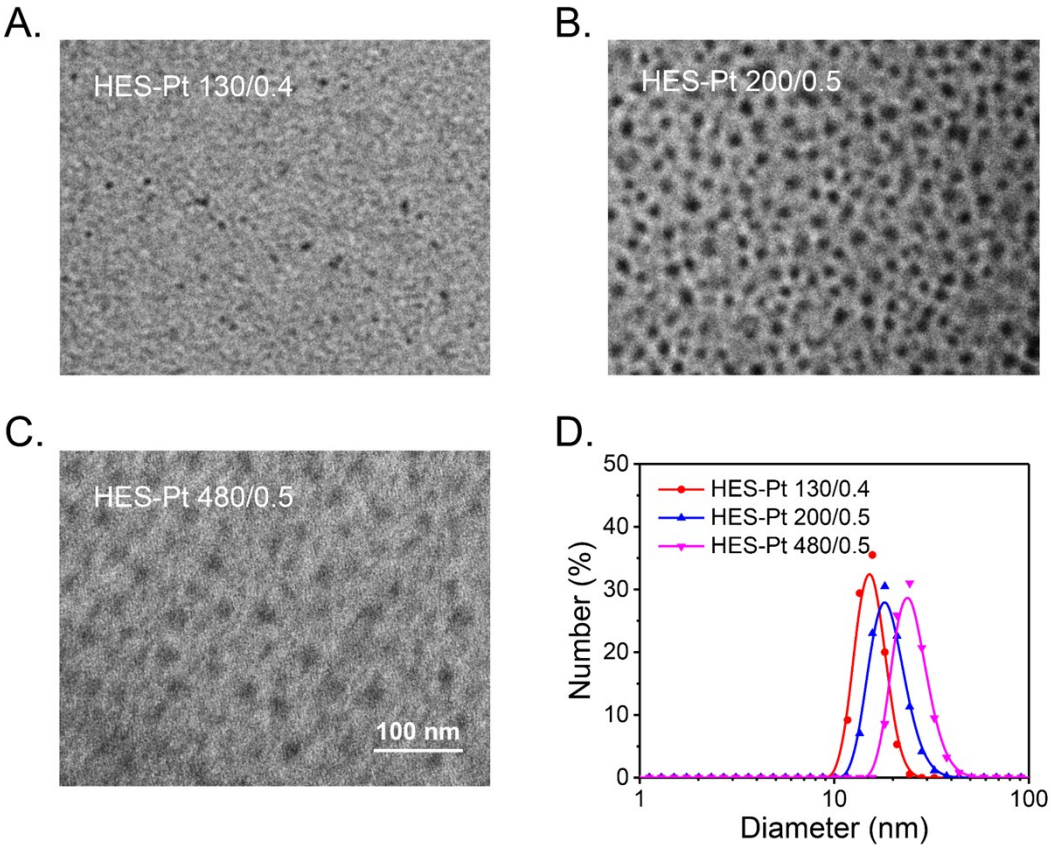

Figure S7. TEM images of HES-Pt (130/0.4) (A), HES-Pt (200/0.5) (B), and HES-Pt (480/0.5) (C). The scale bar is 100 nm for (A), (B), and (C). Size distribution of HES-Pt (130/0.4), HES-Pt (200/0.5), and HES-Pt (480/0.5) measured by DLS (D).

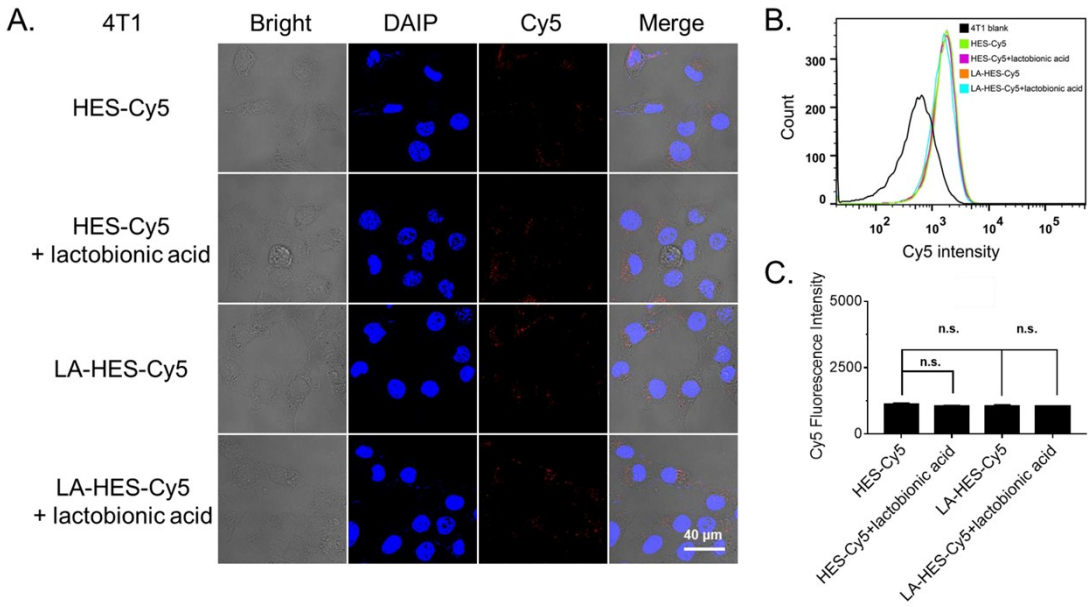

Figure S8. Cellular uptake of HES-Cy5 and LA-HES-Cy5. (A) CLSM images of 4T1 cells incubated with HES-Cy5 and LA-HES-Cy5 for 12 h, and 4T1 cells preincubated with 500 μg/L lactobionic acid for 4 h followed by incubation with HES-Cy5 and LA-HES-Cy5 for 12 h. The scale bar is 40 μm and applied for all images. (B) Flow cytometry analysis of 4T1 cells incubated with HES-Cy5 and LA-HES-Cy5 for 12 h, and 4T1 cells preincubated with 500 μg/L lactobionic acid for 4 h followed by incubation with HES-Cy5 and LA-HES-Cy5 for 6 h. (C) Mean fluorescence intensity determined by flow cytometry

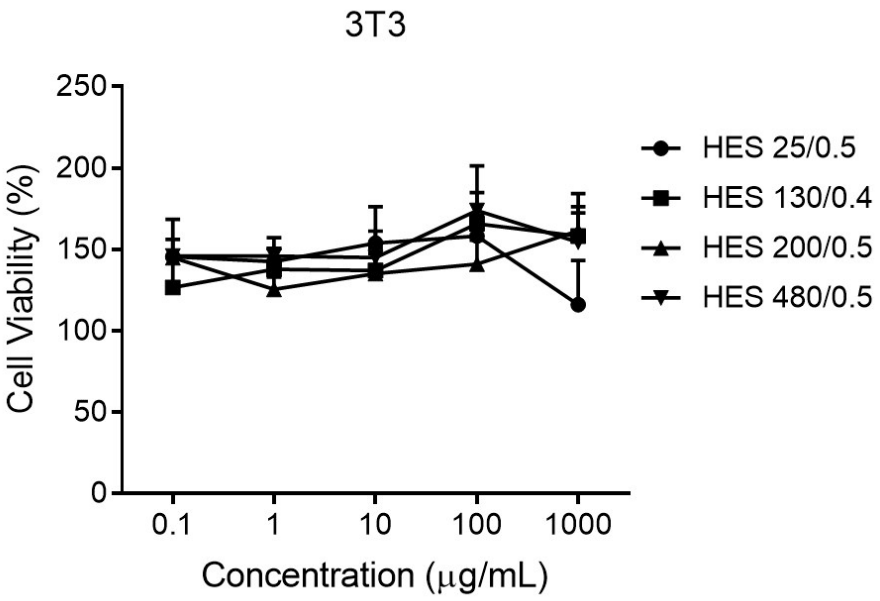

Figure S9. In vitro cytotoxicity of different HES against 3T3 cells.

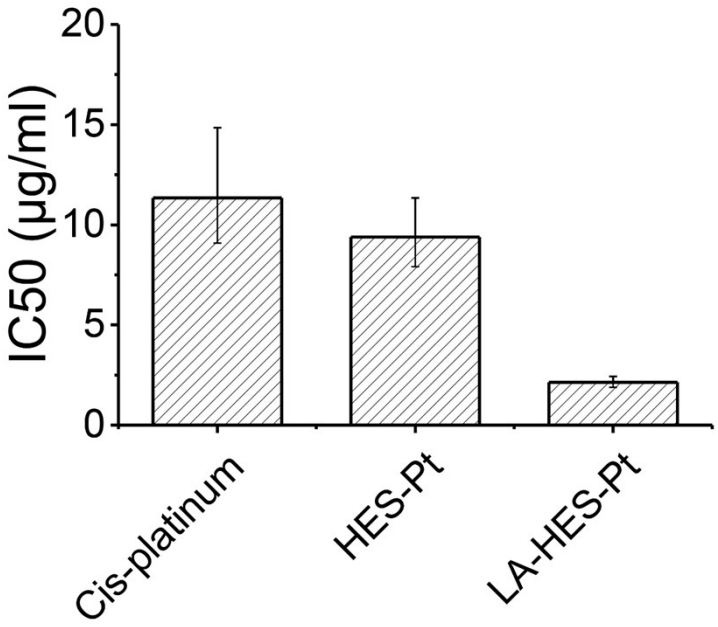

Figure S10. The IC50 value of cis-platinum, HES-Pt and LA-HES-Pt determined by in vitro cytotoxicity experiments with HepG-2 cells.

Table S1. Degree of branching, C_2/C_6 ratio, and molar substitution of hydroxyethyl of different HES determined by ^1H NMR spectra.

Sample	HES 25/0.5	HES 70/0.5	HES 130/0.4	HES 200/0.5	HES 480/0.5
Degree of branching	5.9%	5.5%	6.3%	6.0%	5.9%
C2/C6 ratio	3.2	3.3	3.2	2.9	3.0
MS	0.33	0.35	0.38	0.43	0.49

Table S2. The IC50 value of cis-platinum, HES-Pt and LA-HES-Pt determined by in vitro cytotoxicity experiments with HepG-2 cells.

Sample	IC50 Value (μg/mL)	Confidence interval (μg/mL)
Cis-platinum	11.34	9.087--14.84
Pt-COOH	---	---
HES-Pt	9.394	7.907--11.34
LA-HES-Pt	2.144	1.889--2.425

1. M. D. P. D. M. Westphal, M. D. P. D. Michael F. M. James, M. D. P. D. S. Kozek-Langenecker, M. D. P. D. R. Stocker, M. D. B. Guidet and M. D. P. D. F. F. H. Van Aken, *Anesthesiology*, 2009, **111**, 187-202.
2. K. Sommermeyer, U. Hildebrand, F. Cech, E. Pfitzer, K. Henning and B. Weidler, *Starch - Stärke*, 1992, **44**, 173-179.
3. S. U. Frick, M. P. Domogalla, G. Baier, F. R. Wurm, V. Mailänder, K. Landfester and K. Steinbrink, *ACS Nano*, 2016, **10**, 9216-9226.
4. B. Kang, P. Okwieka, S. Schöttler, S. Winzen, J. Langhanki, K. Mohr, T. Opatz, V. Mailänder, K. Landfester and F. R. Wurm, *Angewandte Chemie International Edition*, 2015, **54**, 7436-7440.
5. E. A. Kamoun and H. Menzel, *Journal of Polymer Research*, 2012, **19**, 9851-9864.
6. H. H. Xiao, R. G. Qi, S. Liu, X. L. Hu, T. C. Duan, Y. H. Zheng, Y. B. Huang and X. B. Jing, *Biomaterials*, 2011, **32**, 7732-7739.
7. R. P. Feazell, N. Nakayama-Ratchford, H. Dai and S. J. Lippard, *J Am Chem Soc*, 2007, **129**, 8438-8439.